Neurotype matching in monogamous rodents is modulated by early-life sleep experience

Lezio S. Bueno-Junior[1]*, Noah E. P. Milman[2,3], Carolyn E. Jones-Tinsley[2,3], Anjesh Ghimire[1], Peyton T. Wickham[2,3], Yujia Hu[4,5], Bing Ye[4], Miranda M. Lim[2,3], Brendon O. Watson[1]*

[1]Department of Psychiatry, University of Michigan Medical School, Ann Arbor, MI, USA

[2]Portland VA Research Foundation, Portland, OR, USA

[3]Department of Neurology, Oregon Health and Science University, Portland, OR, USA

[4]Life Sciences Institute and Department of Cell and Developmental Biology, University of Michigan, Ann Arbor, MI, USA

[5]Lerner Research Institute, Cleveland Clinic, Cleveland, OH, USA

*Correspondence: Lezio S. Bueno-Junior (soaresbl@umich.edu), Brendon O. Watson (brendonw@umich.edu)

Abstract

Studies of human sociability indicate stronger social affinity in matched-neurotype dyads (e.g., two individuals with autism or two without) compared to mixed-neurotype dyads (e.g., one individual with autism paired with one without). Is this neurotype matching phenomenon also quantifiable in non-human animals? Using deep learning tools, we analyzed dyadic male-female interactions in prairie voles, a highly social rodent species. To simulate “neurotypes”, voles were exposed to either control conditions or early-life sleep disruption (ELSD) during a critical neurodevelopmental period (postnatal days 14-21), recapitulating two features of human autism: developmental sleep disruption and later-life atypical sociability. Analogous to human studies, voles showed signs of reduced social affinity in mixed dyads compared to matched dyads, including sex-specific changes in aggression and body orientation toward the conspecific. These findings advance our understanding of social affinity, providing a framework for new studies in both animal models and humans.

Introduction

During social interactions, we may experience feelings of closeness and affinity or, conversely, awkwardness and lack of affinity. Researchers have sought to quantify these feelings of “social chemistry” in humans, often through questionnaires to assess subjective perceptions about the social peers [1–6]. There have also been attempts to track these social properties more objectively in humans by measuring story recall, speech fluency, motion energy, facial expressions, mutual gaze, task cooperation and inter-brain synchrony [7–20].

Most of these human studies have focused on the smallest social unit – the dyad – to assess how the similarity between individuals affects social affinity, or rapport. A common strategy in these studies is to mix and match individuals with different “neurotypes”, especially those with autism spectrum disorders (ASD) or neurotypical controls, forming dyads with matched neurotypes (neurotypical-neurotypical or ASD-ASD) or mixed neurotypes (neurotypical-ASD or vice-versa). Interestingly, mixed dyads have been associated with lower affinity than matched dyads, suggesting that it is not simply the number of neurodivergent individuals in the dyad that modulates sociability [2–6,13,15,17–19]. This aligns with the growing awareness that social difficulties in neuropsychiatric spectra may partly result from interpersonal mismatches, rather than solely from individual traits [21–23].

To explore neurotype matching biologically, we can use rodent models. However, neurotype matching research has limited correspondence in the rodent model literature, despite the existence of established rodent models in social neuroscience, as well as computational ethology tools for tracking groups of animals. Rodent models include ASD-like phenotypes or genotypes (e.g., prenatal valproic acid rat model and Shank3 knockout mouse model) [24,25], which capture some components of sociability but are often limited by the focus on just one animal per assay. In turn, computational ethology tools include whole-body or body-part keypoint trackers (e.g., JAABA, idtracker.ai, DeepLabCut, SLEAP) [26–29], which capture multi-

animal dynamics but fail to identify nuances, like the social role of each individual. Our group has contributed innovations to both areas. For rodent modeling, we have described that early-life sleep disruption (ELSD) impairs adult pair bonding in a monogamous rodent species: the prairie vole (*Microtus ochrogaster*), mimicking the link between developmental sleep issues and altered sociability in human ASD [30]. For computational ethology, we initially published a DeepLabCut-based system to measure body orientation and distance between two spatially-restricted prairie voles [31]. Then, more recently, we co-developed LabGym2: a postural motif tracker that identifies social roles (e.g., “chasing” versus “being chased”) in groups of freely-moving animals, including prairie vole dyads [32].

In the present study, we integrated these innovations to quantify social roles in matched versus mixed prairie vole dyads, drawing a parallel to neurotype matching studies in humans. Specifically, male and female prairie vole pups were exposed to control conditions or ELSD from postnatal days 14-21, a critical neurodevelopmental window. Upon reaching adulthood, these voles were paired into matched or mixed neurotype combinations. Behaviors were then analyzed using long-duration recordings, lasting several hours to days. We found that mixed dyads exhibit altered body orientation behaviors and higher incidence of aggressive bouts, comparable to the lower affinity found previously in mixed human dyads. Furthermore, each behavior in prairie voles varied by sex and followed a different timeline, adding both sex specificity and temporal resolution to the available knowledge from human dyad studies. These findings have implications for both the basic and clinical understanding of social affinity, in addition to offering an analytical framework for future studies in different species.

Results

Overview of animal pairing and behavioral analysis

We utilized two behavioral phenotypes: early-life sleep disrupted (ELSD) prairie voles and age-matched controls (Ctrl), including both sexes. This resulted in four dyad combinations: Ctrl-Ctrl, ELSD-ELSD, Ctrl-ELSD, ELSD-Ctrl (first and second acronyms represent male and female, respectively). The ELSD method was initially validated by our group [30] and is illustrated in **Fig 1A**. Briefly, home cages containing both parents and their pups – postnatal days (P) 14-21 – were placed on orbital shakers for gentle, intermittent agitation (see Methods). The pups were then weaned and housed with same-sex siblings under standard conditions until adulthood, generating cohorts of male and female ELSD voles. Ctrl voles underwent the same conditions, except for sleep disruption with the orbital shaker (**Fig 1A**). Our previous studies [30,33] have shown that ELSD reduces REM sleep time and fragments NREM sleep in prairie vole pups while preserving their body weight, corticosterone levels, and parental care. Subsequent to these acute changes, we have shown that ELSD triggers long-term changes in social affiliation (e.g., partner-directed huddling during tests for pair bond formation), cognitive flexibility, object interactions and neocortical cytoarchitecture, forming a phenotype relevant to human ASD [30,34].

Here, ESLD effects on dyadic behavior are explored more deeply thanks to computational ethology. We describe two strategies. <u>Experiment 1</u>: body-part keypoint tracking (DeepLabCut) [28] of mutually naïve male-female pairs separated by a wire mesh divider (**Fig 1B**). <u>Experiment 2</u>: whole-body behavioral classification (LabGym2) [32] of the same male-female pairs, but without the divider (**Fig 1C**).

<u>Experiment 1: initial divided cohabitation</u> (**Fig 1B**; **S1 Movie**). This experiment consisted of 72-h overhead video recordings where voles interacted through a wire-mesh divider at the

center of the cage. This was the first encounter these animals had with each other. While this setup imposed a physical limitation on social interactions, it yielded uniform postural and spatial measures throughout recordings. This allowed us to decompose these measures into three DeepLabCut-derived variables: body direction to divider, distance to divider and locomotion speed (**Fig 1B**). In a previous study [31], we characterized the sex-specific impacts of ELSD to these variables, including alterations in male body orientation and female circadian activity. However, we did not examine neurotype matching effects in that study; such effects are reported here.

Experiment 2: subsequent undivided cohabitation (**Fig 1C**; **S2 Movie**). This experiment consisted of 4-h overhead video recordings using the same voles, three to four days after Experiment 1, meaning that the opposite-sex mates had already been exposed to each other at the time of Experiment 2, i.e., dyad assignments were preserved between experiments (see Methods). In this setup, the animals were allowed to engage in freely moving partner-referenced behaviors without a divider. This resulted in an enriched behavioral repertoire, which is more difficult to analyze with DeepLabCut but amenable to newer LabGym2-based behavioral classification (**Fig 1C**). One novel aspect of LabGym2 – a software that we co-developed [32] – is the ability to categorize the social role of each individual (e.g., “chasing” versus “being chased”). We utilized this capability in combination with manual validation to ensure reliable identity tracking and sex specification per behavior. This resulted in the labeling of five behavior categories: *chasing*, *attacking*, *pointing*, *behaving alone*, and *huddling* (**Fig 1C**). Here, “*pointing*” combines sniffing behaviors with a freezing-like behavior that we often observed after each aggressive bout (see **S2 Movie**). See Methods for details.

Therefore, our two experiments yielded very different analyses. Nevertheless, neurotype matching effects emerged in both experiments, as reported below.

129 ***Experiment 1: Mixed dyads showed exacerbated sex differences in body orientation***

130

131 In Experiment 1, male and female interacted through a wire-mesh divider. **Fig 2**
132 describes these interactions over 72 h (1-h bins, see x-axes), with graph columns displaying
133 DeepLabCut-derived behavioral decomposition variables. **Fig 2A** starts by comparing sexes
134 irrespective of dyad grouping. When analyzing direction to divider, we found that male voles
135 spent significantly more time facing toward the divider than females throughout the recording.
136 For distance to divider, both sexes preferred areas near the divider (4-6 cm) during the initial 12
137 h of recording; this variable later plateaued at around 6 cm (halfway between divider and
138 opposite cage wall), suggesting habituation. For locomotion speed, both sexes exhibited higher
139 locomotion in the initial 12 h of recording; this variable later stabilized to lower basal levels, also
140 suggesting habituation (**Fig 2A**). These results corroborate our previous findings [31] that sex-
141 specific body orientation patterns persist even after voles habituate to the environment, as
142 indicated by the stabilization of locomotion and area preference after the initial 12 h. See **Table**
143 **1** for statistics and **S1 Movie** for representative behaviors.

144 By parsing these sex differences into dyad types, we begin to reveal the novel findings
145 of this study. **Fig 2B** shows that while sex differences in direction to divider were significant in
146 both matched and mixed dyads, these differences were more pronounced in mixed dyads and
147 persisted for 72 h (**Table 1**). **Fig 2C** further divides male and female voles into the four juvenile
148 sleep status combinations. In this case, sex differences in direction to divider were significant
149 only in mixed dyads (Ctrl-ELSD, ELSD-Ctrl). Matched dyads, including Ctrl-Ctrl and ELSD-
150 ELSD, showed no significant sex differences (**Table 1**). These results indicate that body
151 orientation behaviors did not change linearly with the number of ELSD individuals in the dyad;
152 rather, neurotype matching was the main factor modulating body orientation.

153 Additional sex differences were specific to mixed dyads and confined to more localized
154 time periods. We observed that ELSD females in Ctrl-ELSD dyads maintained a greater

distance from the divider more than 36 hours into the session, while Ctrl females in ELSD-Ctrl dyads exhibited higher locomotion speed during the initial 12 hours compared to males (**Fig 2C**). However, these sex differences were modest compared to the prominent results in direction to divider (**Table 1**). **Fig 2D** further highlights direction to divider as a sensitive variable, this time comparing matched and mixed dyads within each sex. Males spent significantly more time toward the divider in mixed compared to matched dyads, indicating heightened female-directed orientation in mixed-dyad males (**Table 1**).

Overall, **Fig 2** shows that a supra-individual factor (neurotype matching) preferentially modulated one behavioral component (body direction) in one sex (males). Next, we describe that neurotype matching remained an important factor in a different environment.

Experiment 2: Mixed dyads showed higher female-to-male aggression

In Experiment 2, the wire mesh divider was not present, and animals were able to interact in an unrestricted fashion. **Fig 3** is structured similarly to the results above, with two differences: the recordings lasted 4 h (3-min bins, see x-axes) and the graph columns show LabGym2-based behavior categories. We again start by comparing sexes irrespective of dyad grouping in **Fig 3A**. The social roles of *chasing* and *attacking* were significantly more prevalent in female voles, especially in the first hour of recording (insets), after which these variables decayed to lower basal levels. The social role of *pointing*, which included sniffing and other behaviors (see Methods), was evenly distributed across sexes and showed a more gradual decline over the 4-h period (see lower F values in effects of time in **Table 2**). The role-unspecific categories of *behaving alone* and *huddling* (i.e., behaviors that considered the full dyad, see Methods) also showed gradual time courses, but in opposite directions: *behaving alone* decreased, while *huddling* proportionally increased over time (**Fig 3A**). In addition, *behaving*

180 *alone* and *huddling* were the most frequent behaviors across **Fig 3**, as indicated by the
181 probability axes. See **Table 2** for statistics.
182 Despite their lower occurrence rate, *chasing* and *attacking* are the behaviors with the
183 greatest differential trajectories across types of dyads. As shown in **Fig 3B**, female voles were
184 more likely to chase and attack the males in mixed than matched dyads (**Table 2**). Consistently,
185 in dyad subgroups (**Fig 3C**), female-to-male *chasing* and *attacking* were more frequent in both
186 Ctrl-ELSD and ELSD-Ctrl dyads (**Table 2**). Matched ELSD-ELSD dyads showed no sex
187 differences in *chasing* and a comparatively small difference in *attacking* (**Table 2**), reinforcing
188 that these behaviors did not change linearly with the number of ELSD individuals in the dyad,
189 similar to the findings in dyads behaving across a divider. Additional sex differences were
190 observed in *attacking* (Ctrl-Ctrl) and *pointing* (ELSD-ELSD) (**Fig 3C**), but these were also
191 modest compared to the sex differences in *chasing* and *attacking* behaviors found in mixed
192 dyads (**Table 2**). Furthermore, **Fig 3D** shows within-sex comparisons between dyad types,
193 confirming that mixed-dyad females were more likely to chase and attack than matched-dyad
194 females. No dyad type differences were observed in the other behaviors, i.e., *pointing*, *behaving*
195 *alone* and *huddling* (**Fig 3D-E**; **Table 2**), again highlighting female-to-male *chasing* and
196 *attacking* as the most sensitive behaviors in this analysis.
197 Therefore, neurotype matching preferentially modulated female-to-male aggression in
198 the undivided cage. Below we link Experiments 1 and 2 via correlations within dyads.
199
200 ***Linking divided cohabitation to undivided cohabitation: Neurotype matching affected***
201 ***correlations among behaviors***
202
203 The same dyad assignments were used in Experiment 1 (first male-female encounter
204 and 72-h divided cohabitation) and Experiment 2 (second encounter and 4-h undivided
205 cohabitation), with an interval of three to four days between experiments. This gave us the

206 opportunity to quantitatively link these experiments. Thus, we averaged all behavioral variables
207 per animal (three variables from Experiment 1, five from Experiment 2) and explored linear
208 correlations among such variables. **Fig 4A-B** illustrates correlations between direction to divider
209 in Experiment 1 and all behavioral categories of Experiment 2. Each data point in **Fig 4A-B** is
210 an individual animal. Separate analyses were performed per sex and major dyad type (see
211 Methods).

212 Significant correlations were restricted to female voles and differed between matched
213 versus mixed dyads (**Fig 4B**; see plots with gray background). *Chasing*: positively correlated
214 with direction to divider in mixed. *Attacking*: negatively correlated with direction to divider in
215 matched. *Behaving alone*: negatively correlated with direction to divider in matched. *Huddling*:
216 positively correlated with direction to divider in matched (**Fig 4B**). Thus, a female that oriented
217 more toward the divider in Experiment 1 was more likely to engage in different behaviors in
218 Experiment 2 depending on the dyad type: affiliative behaviors in matched, chasing behaviors in
219 mixed. This suggests that, depending on the dyad type, the same behavior in Experiment 1
220 (body orientation) may have been driven by a different underlying state. **Fig 4C** presents
221 correlation matrices for all variable pairs, providing a comprehensive view of both sex and dyad
222 type differences. The leftmost columns in each matrix of **Fig 4C** (direction to divider) contain the
223 correlations emphasized above. Other correlations were found within each experiment,
224 including negative correlations between alone and huddling, consistent with their opposing
225 trends in Experiment 2 (**Fig 3**).

226

227 ***Female-to-male behavior transitions differed between matched and mixed dyads***

228

229 The analyses above ignore within-dyad actions and reactions at finer temporal scales.
230 How likely is behavior B in vole 2 after behavior A in vole 1? Do these likelihoods change with
231 dyad type and/or sex directionality (male-to-female, female-to-male)? In **Fig 5** we explore these

232 questions using behavior transition probabilities, thus capturing temporal sequence patterns
233 from each dyad type and sex directionality. Data from the video frames were divided into 1-s
234 time bins; this temporal resolution was deemed optimal to capture all transitions between
235 behaviors, including to and from aggression bouts – the quickest behaviors in our dataset (**S2**
236 **Movie**). We then conducted this analysis separately per major dyad type (matched, mixed) and
237 sex directionality (male-to-female, female-to-male).

238 **Fig 5A-B** shows data from Experiment 1 (divided cohabitation). The most informative
239 variables in that dataset – direction and distance to divider – were continuous and therefore
240 required discretization prior to transition analysis. Thus, we discretized direction to divider into
241 "toward" or "opposite", and distance to divider into "near" or "away", resulting in four categories:
242 *toward-near*, *opposite-near*, *toward-away*, *opposite-away* (see Methods). The directed graphs in
243 **Fig 5A** illustrate transitions among these categories, averaged across dyads. The edges
244 represent probabilities, coded by line width and grayscale (**Fig 5A**). For this analysis, we
245 focused on the initial 12 h of the 72-h recording, when the animals were more active (**Fig 2**).

246 The main visual pattern in all graphs is the convergence to, and recurrence of, *toward-*
247 *near* (black edges): these represent the highest transition probabilities in both sex
248 directionalities (**Fig 5A**). Particularly in the male-to-female graphs, the convergence to, and
249 recurrence of, *opposite-near* (dark gray edges) also showed relatively high probabilities. All
250 other transitions were less likely (light gray edges) (**Fig 5A**). The more distributed patterns in the
251 male-to-female graphs indicate higher variation: female voles were more active and rotated
252 themselves more (**Fig 2**, **S1 Movie**), thus increasing the chances of male behaviors being
253 followed by both body orientation categories in the females. In contrast, the female-to-male
254 graphs indicate lower variation: all female behaviors were more likely followed by *toward-near* in
255 the males, simply because this behavior was predominant in males (**S1 Movie**).

256 Of interest to this study, we found differences between matched and mixed dyads,
257 specifically in female-to-male transitions. For quantification, transition probability matrices were

258 calculated per dyad, reshaped into dyad x edge matrices (edges were used as repeated
259 measures), and compared between matched and mixed dyads, resulting in **Fig 5B** (self-loops
260 were excluded; see Methods). In mixed dyads, two female-to-male transitions were more likely:
261 *opposite-near* to *toward-near* and *toward-away* to *toward-near* (**Fig 5B**). We interpret that this
262 was driven by the tendency of mixed-dyad males to spend more time toward the divider, as
263 reported earlier (**Fig 2**). In matched dyads, three female-to-male transitions were more likely:
264 *toward-near* to *opposite-away*, *opposite-away* to *opposite-near*, and vice-versa for the latter (**Fig**
265 **5B**). These re-orientation patterns between male and female were infrequent (see light gray
266 edges in **Fig 5A**) but could be speculated as body posture signals. **Fig 5B** additionally contains
267 examples of the distributions behind each behavior pair, shown here as mean +/- standard
268 deviations (each data point represents a dyad). See **Table 3** for statistics.
269 **Fig 5C-D** shows the same analysis, but from the full 4 h of Experiment 2 (undivided
270 cohabitation), with five labeled behaviors during free interaction. As illustrated by the average
271 directed graphs in **Fig 5C**, the highest transition probabilities were found in the recurrence of
272 *behaving alone* and *huddling* (black self-loops). This was expected, as *behaving alone* and
273 *huddling* were both prevalent and self-sustaining, as shown previously (**Fig 3**). For
274 quantification, we excluded such loops to focus on the behavior pairs, as described above,
275 resulting in **Fig 5D**. In mixed dyads, two female-to-male transitions were more likely: *huddling-*
276 *to-chasing* to *alone-to-pointing* (**Fig 5D**). This could reflect higher activity overall in mixed dyads,
277 including shorter and more intermittent periods of huddling and more frequent alone-to-pointing
278 re-encounters. However, these transitions showed very low probabilities (hardly visible in **Fig**
279 **5C**; see also y-axes in **Fig 5D**) and thus we interpret them cautiously. A more robust
280 observation was that female-to-male *chasing-to-huddling* was more likely in matched dyads (**Fig**
281 **5D**). Thus, female chasing in matched dyads was possibly more affiliative, or huddling-seeking
282 (**S2 Movie**). This suggests the existence of different states underlying the same behaviors
283 depending on dyad type, echoing an interpretation we proposed in the previous subsection.

Therefore, aside from the specificities of each behavior pair, **Fig 5** shows that neurotype matching influences actions and reactions on the scale of seconds, reinforcing the time series and correlation analyses reported earlier.

Discussion

We utilized algorithms for annotation and decomposition of social behaviors to examine neurotype matching in rodents. Opposite-sex prairie voles were assigned to either matched or mixed-neurotype dyads, resembling human studies involving ASD. The voles were then filmed in two experiments: initial divided and subsequent undivided cohabitation recordings. Dyad type effects emerged from both experiments in a correlated manner, suggesting robust underlying mechanisms. Our observations varied by sex and spanned multiple temporal scales, including body orientation patterns over days, incidence of aggression over hours, and behavioral transitions over seconds. These findings might influence further development of behavioral paradigms and studies integrating social behavior and physiology.

Juvenile sleep and atypical sociability

Neurotype matching studies in humans often involve mixing and matching neurotypical and neurodivergent individuals, especially those with ASD [2–6,13,15,17–19]. Here, “neurodivergent” corresponds to adult prairie voles exposed to ELSD during post-natal days 14-21, a method described previously by our group [30,33]. ELSD causes fragmentation of non-rapid eye movement sleep (NREM) and reduces both duration and gamma power of rapid eye movement sleep (REM), as recorded electrographically from prairie vole pups. Body weight, corticosterone levels, and parental care are all unaffected by ELSD, indicating that this method selectively targets juvenile sleep physiology [30,33]. Despite this selectivity, ELSD provokes

310 long-lasting behavioral and neurobiological alterations into adulthood. Behavioral alterations
311 include impaired cued fear extinction and reduced male-to-female partner preference
312 expression. Neurobiological alterations include cytoarchitectural markers of excitatory-inhibitory
313 imbalance in brain regions involved in sensory and cognitive processing, such as increased
314 expression of inhibitory neurons in somatosensory cortex, as well as increased dendritic spine
315 density and decreased presynaptic glutamate labeling in prefrontal cortex [30,34]. Similar
316 neurobiological changes are present in human ASD, making prairie vole ELSD relevant for
317 investigating ASD and other disorders linked to poor juvenile sleep [35].

318 As reviewed previously [35–37], sleep disruption during infancy has been associated
319 with ASD in humans. Brain maturation processes in humans, such as axonal myelination and
320 synaptic pruning, depend on healthy sleep during development. Disrupted sleep may interfere
321 with these processes and increase vulnerability to ASD-like symptoms, including social
322 difficulties [35–37]. Since neurotype matching modulates behavior in both prairie vole ELSD
323 (present study) and human ASD [2–6,13,15,17–19], we can speculate that some of these social
324 properties may trace back to sleep quality during development. This is, of course, a more
325 complex question. First, the relationship between sleep disruption and ASD is recognized as a
326 bidirectional and multifaceted comorbidity, with sleep disturbances both amplifying and being
327 amplified by ASD [36,37]. Second, human ASD is linked with other factors not directly related to
328 sleep, such as heritability and perinatal exposure to toxicants [38]. And third, juvenile sleep is
329 sensitive to circumstances not directly related to ASD, such as respiratory problems and
330 household conditions [39,40]. All these factors can lead to (and interact with) ASD [41], making
331 it difficult to isolate the role of juvenile sleep in ASD, let alone dyad type properties. Still, our
332 results suggest that juvenile sleep does play a role in these social properties – a role that we
333 found to be discernible in non-human animals, despite the elusive mechanisms. Future studies
334 could disentangle poor juvenile sleep from other environmental and genetic factors using

335 different rodent models, furthering the study of non-human neurotype matching and
336 complementing human ASD research.
337
338 ***Markers of social affinity across neuropsychiatric spectra***
339
340 Human ASD encompasses a myriad of features, including subtle presentations of ASD,
341 which can be challenging to detect and often go undiagnosed [42,43]. Likewise, ELSD prairie
342 voles do not show overt behavioral changes. In our experience, these changes can only be
343 detected with quantification, whether using manual [30] or computerized [31] tracking. Thus,
344 ELSD prairie voles might represent a nuanced ASD-like spectrum, analogous to nuanced
345 neuropsychiatric spectra in humans. Our experiments add complexity to this question. Despite
346 the elusive nature of these spectra, their phenotypes can still supply us with controllable
347 "reagents" to manipulate "social chemistry". The "purity" of these reagents (i.e., phenotypes)
348 certainly vary among species or between laboratory and naturalistic settings, yet they still seem
349 to bring about some form of chemistry, as suggested by the literature on human dyads and our
350 study in prairie voles. Furthermore, dyadic behavior in humans has been investigated beyond
351 ASD, including studies on dysphoria, attention deficit disorder, and decision making [1,7–9], all
352 of which reinforcing that mixing or matching different phenotypes (or social styles) can modulate
353 behavioral performance and sociability. This indicates that social matching properties are
354 measurable across species and phenotypes, with implications for basic science, mental health,
355 and a better understanding of reciprocity and empathy [21–23].
356 These questions warrant further investigation using data-intensive metrics of social
357 affinity. Recent human ASD studies involving matched and mixed dyads used objective metrics
358 from video, audio and electroencephalography, including motion energy, mutual gaze,
359 backchanneling, verbosity, smile synchrony, and inter-brain synchrony [12,13,15,17,18].
360 Generally, these studies also support neurotype matching properties, though some metrics are

361 inconsistent with this trend. Such inconsistency might be attributed to low temporal resolution,
362 as these studies used aggregated metrics across sessions when comparing dyad types. Time
363 series analyses, like those here, could be employed in future studies to extract detailed
364 information from each metric, potentially identifying optimal metrics for real-time sociability
365 tracking and translatability across species. Other human dyad studies, unrelated to ASD or
366 neurotype matching, used additional metrics, including task cooperation, motor coordination,
367 smell-induced arousal, and functional brain imaging or spectroscopy [14,20,44–49]. This variety
368 of methods suggests promising avenues for studying dyadic behavior across species and
369 neuropsychiatric disorders.
370
371 ***Sex differences and ethological nuance***
372
373 In our male-female grouping design (Ctrl-Ctrl, ELSD-ELSD, Ctrl-ELSD, ELSD-Ctrl) we
374 considered both sex and dyad type. This revealed dyad type effects both between and within
375 sexes in prairie voles. Between-sex and within-sex interactions have also been recognized in
376 human ASD. Core ASD traits seem to vary equivalently between sexes (e.g., communication
377 impairments, repetitive behaviors), whereas associated ASD traits seem to vary independently
378 within each sex (e.g., hyperactivity in males, depression in females) [50–52]. To our knowledge,
379 these sex-related variables have not been experimentally manipulated in studies on neurotype
380 matching and ASD. As shown here with prairie voles, sex differences in body direction (males
381 spent more time toward the divider) and aggression (females chased and attacked more) were
382 exacerbated in mixed dyads. We can now speculate that neurotype matching could also amplify
383 sex differences in humans and other species. Investigating these questions could provide
384 deeper insight into sex differences in human ASD or ASD-like models.
385 Moreover, we found that female body orientation in divided cohabitation (Experiment 1)
386 led to different outcomes in undivided cohabitation (Experiment 2) depending on the dyad type:

increased affiliation in matched dyads (less attacking, more huddling) and decreased affiliation in mixed dyads (more chasing, less chasing-to-huddling transitions). Therefore, a female behavior that looked the same – body direction – may have been driven by different underlying states depending on the dyad type, e.g., female body direction was possibly more huddling-oriented in matched dyads. Interestingly, these states in females may have influenced (and been influenced by) the males. In mixed dyads, males spent more time toward the divider in Experiment 1, and once the divider was removed in Experiment 2 the females attacked more frequently. Thus, females may have reacted proportionally to the males' approaches upon removal of the divider, which could be another explanation why aggression was more frequent in mixed dyads. Aggressivity, affiliation and other behavior types (e.g., courting, foraging) are indeed recognized to vary with sex, social hierarchy and environmental context [53–55], suggesting an interplay between internal and expressed states. We propose that matching and mixing rodent "neurotypes" like we did here is a promising approach to investigate these states.

Concluding remarks

This study reveals that neurotype matching is a quantifiable phenomenon in rodents. As computational ethology continues to optimize social behavior tracking, the emergent properties of social groups may become more tangible. This progress may reshape behavioral paradigms, from dyad-based studies to freely moving partner preference studies, strengthening the link between animal models and human sociability.

408 **Materials and methods**

409

410 ***Subjects***

411

412 Prairie voles (n = 28 each sex) were sourced from a genetically diverse pool of 13
413 breeders in an accredited, fully-contained laboratory facility (VA Portland Health Care System).
414 Litters containing both male and female sibling pups (2-9 pups each breeder pair) were raised
415 with their parents (no cross fostering) until post-natal day 21 (P21). During the P14-21 period,
416 specifically, the litters were subjected to either control (Ctrl) or early-life sleep disruption (ELSD)
417 conditions (details below). At P21, pups were weaned into same-sex sibling groups and
418 remained at the same vivarium until approximately P90. The sibling groups were then shipped
419 to the University of Michigan Medical School for the primary recordings of this study.
420 Consistent housing conditions were maintained across both institutions, including 14:10
421 h light/dark cycle (lights on at 5:00 am), temperature (20-23 °C), ventilation (double-filtered
422 outside air, negative pressure), humidity (30-70%), bedding (rolled paper pellets), environmental
423 enrichment (cotton nestlets and wooden blocks/sticks) and *ad libitum* water and food (rabbit
424 chow, corn, cracked oats). Each week, the animals were transferred to a new cage with fresh
425 bedding and enrichment. All procedures in this study were approved by the Institutional Animal
426 Care and Use Committees (IACUC) of VA Portland Health Care System (protocols 6069 and
427 3652) and University of Michigan Medical School (protocol 00011423).
428 Our animals originated from a colony at Emory University, itself derived from wild-
429 captured animals in the State of Illinois, USA. To preserve genetic diversity, bi-annual
430 exchanges of animals occur among several institutions, including North Carolina State
431 University, University of California Davis, University of Colorado Boulder, and Florida State
432 University.

433

434 ***Early-life sleep disruption***

435

436 Prairie vole ELSD phenotypes of both sexes were generated by placing home cages
437 with P14-21 pups and their parents on an orbital shaker for intermittent gentle agitation (10
438 seconds on, 100 seconds off, 110 rotations per minute). ELSD animals were provided hydrogel
439 instead of water bottles to prevent water spillage during agitation. Ctrl animals experienced the
440 same conditions except for agitation (**Fig 1A**). As previously described by our group [30,33,34],
441 ELSD disturbs sleep in prairie vole pups without affecting their hormonal markers of stress, or
442 the parental care they receive. The acute effects of ELSD are, therefore, confined to sleep
443 electroencephalography (EEG) parameters, including fragmentation of NREM sleep and
444 reduction of REM sleep time by more than 20% over a 24-hour period [30]. Given this support
445 from our previous studies, here we used identical cage agitation parameters without EEG
446 validation, resulting in a non-invasive (purely behavioral) experimentation timeline.

447

448 ***Dyad assignment and age at recording***

449

450 Following the ELSD or Ctrl procedures at P21, the pups were weaned into same-sex
451 groups of 2-4 siblings per cage until adulthood, resulting in four types of sibling groups (Male-
452 Ctrl, Male-ELSD, Female-Ctrl, Female-ELSD). Sexually naïve opposite-sex adults were then
453 randomly assigned into matched dyads [Male-Ctrl/Female-Ctrl (n=7), Male-ELSD/Female-ELSD
454 (n=8)] or mixed dyads [Male-Ctrl/Female-ELSD (n=7), Male-ELSD/Female-Ctrl (n=6)] prior to
455 recordings, for a total of 28 dyads (**Fig 1A**).

456 Our recording setup could accommodate up to four dyads at a time (details below).
457 Since there were 28 dyads in total, the recordings were divided into seven cohorts of four
458 dyads. Furthermore, an interval of 2-3 weeks was necessary between cohorts due to the
459 duration of the experiments combined with preparatory activities, like cage cleaning and file

management. This resulted in a four-month period to record all 28 dyads. Thus, the ages of the animals at the time of recording varied with a mean +/- standard error of 185.8 +/- 6.5 days of age. However, the individuals of each dyad were still age-matched, with an age difference of 11.1 +/- 2.2 days, randomly distributed across dyad types.

Recording setup

For recording, we developed a vibration-free optomechanical assembly using metal parts from a vendor (ThorLabs), as described previously [31]. This setup holds two infrared-sensitive grayscale cameras (Basler, acA1300-60gm) positioned at 90° overhead angle. Each camera was mounted to a fixed focal length lens (Edmund Optics, 6 mm UC Series) and surrounded by four infrared LED illuminators. Each camera/lens was able to frame two home cages, hence the ability to record four dyads at a time. This system was installed in a room with light/dark phases, which however did not affect imaging brightness, as it relied on infrared reflectance. The cameras were connected to a computer via a network adapter (Intel Pro 1000/PT), and data were stored on a redundant array of independent disks (RAID). Recording settings were configured via Pylon software (Basler) with the following parameters: 8-bit grayscale depth, frame width x height of 800 x 896 pixels, no binning, 1328 kbps data rate, 20 Hz frame rate. Exposure and brightness were adjusted prior to each recording by manipulating the lenses and infrared illuminators, without digital adjustments. Data were acquired into mp4 files (H.264 coded) using StreamPix software (NorPix). For the 72-h recordings of Experiment 1, specifically, recordings were acquired into 6-h mp4 files to ensure file readability, including 2-s margins at the beginning and end of each 6-h file.

486 ***Experiments 1 and 2***

487

488 Experiment 1 consisted of divided cohabitation for 72 h starting at 8 am, i.e., 3 h after the
489 onset of the light phase. Each male-female pair was placed in a bedded home cage (48.3 cm
490 length, 25.4 cm width, 20.3 cm height) with a lab-made divider at the center of the cage. Thus,
491 each animal was spatially restricted to a quadrant, producing uniform behavioral variables
492 across recordings (**Fig 1B**). The dividers were made of metal wire mesh (square mesh, 6.5 mm
493 aperture, 22 cm wide, 28 cm high) covered on both sides with clear polycarbonate sheet (0.5
494 mm thick) to prevent animals from climbing. The bottom section of the metal mesh, measuring
495 6.5 cm in height, was left exposed without the polycarbonate sheet, allowing animals to
496 exchange bedding, smell each other and engage in face-to-face and body-to-body interactions.
497 Chow and gel were placed at consistent locations away from the divider, on the left and right
498 sides of the animal, respectively. No environmental enrichment objects were provided,
499 encouraging the animals to interact. A handwritten label was placed outside each quadrant
500 displaying animal metadata (sex, ELSD vs. Ctrl, quadrant number), clearly visible in each
501 recording for extra documentation. Cardboard barriers were placed between adjacent cages,
502 preventing different dyads from seeing each other during the multi-dyad recordings.
503 Experiment 2 consisted of undivided cohabitation for 4 h, also beginning at 8 am, 3-4
504 days after the end of Experiment 1; animals were single-housed at the vivarium between
505 experiments. Before each recording of Experiment 2, the male and female were placed in the
506 same home-cage quadrants, with the same handwritten label, same bedding and without chow
507 or gel. We then removed the divider *while recording*, ensuring animal traceability throughout the
508 recording, as male and female lacked physical differentiators (**Fig 1C**). See the next section for
509 further identity verification methods. The male and female were then allowed to interact freely.
510 At the end of the recording, each animal was visually inspected to confirm sex, resulting in a
511 100% match with the original metadata.

512 ***Data pre-processing and animal tracking***

513

514 For Experiment 1, each camera recorded two divided cages and, therefore, four
515 quadrants, one animal per quadrant. Thus, we decided to crop each video into four smaller
516 videos (384 x 416 pixels), one per quadrant, using Adobe Premiere and Media Encoder. By
517 doing this we eliminated the need for identity verification in Experiment 1 (unlike Experiment 2,
518 as described below). The cropped videos were then processed through DeepLabCut, a
519 supervised keypoint tracker [28]. A resnet-50 network was used to label seven keypoints per
520 animal: nose, left/right ears, three locations along the "spine", and tail base (**Fig 1B**; **S1 Movie**).
521 The network was trained with video frames from three males and three females, each frame
522 representing varying levels of difficulty: from clear imaging of the animal (without obstruction of
523 body parts) to challenging situations (e.g., curled posture when sleeping or eating, tail base
524 hidden under bedding, nose hidden by the mesh divider). The network was trained using a
525 laboratory server (CPU: Intel Xeon E5-2640 v3 @ 2.60 GHz. RAM memory: 512 GB. GPU:
526 NVIDIA GeForce GTX 1080 Ti) and deployed to unseen (held-out) data. Once keypoint
527 coordinates were generated for each recording, we proceeded to behavioral decomposition
528 analysis using MATLAB (MathWorks), as detailed in the next section.

529 For Experiment 2, all video processing and behavior annotation steps were performed
530 using LabGym2, an open-source machine vison tool that we co-developed (including authors:
531 Y.H., B.Y., and L.S.B-J.) [32]. First, each raw video was cropped into two rectangular videos
532 (800 x 450 pixels), one per cage, so that each video contained one male-female dyad. The
533 cropped videos were then contrast-enhanced to highlight the animals against the background
534 (bedded cage). These videos were then analyzed using two neural networks that we trained
535 during our previous study: *Detector* and *Categorizer* [32]. Step 1: Segmentation and masking of
536 each animal using the *Detector*. Step 2: Mask-based foreground extraction to obtain the raw
537 pixels of each animal; background pixels were set to zero (black). Step 3: Unsupervised tracking

538 of masks over consecutive frames based on foreground appearance and distance. Step 4:
539 Generation of spatiotemporal patterns as inputs for the *Categorizer*, including body contour
540 outlines around the animals. Specifically for the focal animal, these outlines were color-coded
541 from blue to red to indicate the temporal progression of movements within groups of frames, i.e.,
542 time bins totaling 0.67 s per bin. The non-focal (or reference) animal was color coded in a fixed
543 tone of gray (**Fig 1C**). The focal and reference roles were alternated per animal by processing
544 each recording twice, enabling social role identification [32]. Time bin size (0.67 s) was
545 determined to match the timescale of prairie vole behavior, including quick bouts of chasing and
546 aggression. Step 5: Categorization of spatiotemporal patterns into behaviors (**Fig 1C**). This step
547 involved manual sorting of behavioral examples – the primary supervised aspect of LabGym2 –
548 followed by deep learning of the spatiotemporal features of these behaviors using a custom
549 neural network structure, as detailed in our software publication [32]. LabGym2 was run
550 remotely on the University of Michigan Great Lakes cluster. The sessions on this cluster were
551 configured with the following resources: 2.9 GHz Intel Xeon Gold 6226R with 372 GB RAM,
552 NVIDIA A40 with 48 GB VRAM.

553 LabGym2's publication included a proof-of-concept study for prairie vole dyads,
554 demonstrating 100% accurate individual animal tracking throughout each recording [32].
555 However, the recordings in that study were relatively short (10 min), whereas the recordings in
556 the present study were longer (4 h), which we found to increase susceptibility to identity
557 switching. Tracking identities over extended periods (e.g., several hours) indeed remains a
558 challenging task in the field of computational ethology, despite the development of various
559 approaches to multi-animal tracking [26–29]. In our experience, species-typical huddling
560 behaviors exacerbated the risk of identity switching, especially 2-3 hours into the recording,
561 when the voles tended to huddle more. Thus, we chose to identify male and female *manually*,
562 independently on LabGym2's behavioral categorization. Additionally, we leveraged this manual
563 inspection effort to annotate "attacking" and "being attacked" events (**S2 Movie**), which we could

not reliably automate in the current dataset. The annotation of “chasing” and “being chased”, on the other hand, was fully automated, serving as a control for our findings on sex-specific aggression roles. For the manual annotation of animal identities and aggression roles we used the graphical user interface (GUI) of another software tool: DeepEthogram [56].

In summary, we employed two distinct machine vision pipelines in this study, each tailored to a recording environment (divided and undivided cohabitation). However, our study also involved significant human supervision, including manual validation of sex identities and aggression roles, mitigating the risk of over-automation [57]. In fact, our results on “chasing” and “attacking” supported each other (**Fig 3**), which is an important control, as “chasing” and “attacking” were annotated by computer and human, respectively. We believe that human-in-the-loop strategies like these will continue to offer a balance between effort cost and ethological validity, revealing meaningful patterns like the neurotype matching effects reported here.

Behavioral decomposition and categorization

Experiment 1: Keypoints from DeepLabCut represented each animal as an arrow-shaped “skeleton”, one per video frame (**Fig 1B**). The coordinates for these keypoints were imported into MATLAB, converted from pixels to centimeters, and processed into three behavioral variables.

1) Direction to divider: a line was fitted between the extreme keypoints (nose and tail base), and the angle of this line relative to the horizontal plane of the frame was calculated. This angle was then rescaled from -1 (opposite from the divider) to +1 (toward the divider), with clockwise and counterclockwise directions treated equally.
2) Distance to divider: horizontal distance between the center of the animal and the divider, regardless of its position along the vertical axis.

3) Locomotion speed: difference (hypotenuse) between the center of the animal in frame n and frame n+1.

These measures were timestamped according to clock time, in number of seconds x number of frames. The clock was not restarted at midnight, assigning each frame to a unique temporal identifier across the 72 hours. This allowed us to trim and align the recordings to a common 72 h axis, as safety margins of a few minutes were recorded before and after each session. Clock time information was obtained from file naming metadata through the acquisition software (StreamPix, NorPix). These procedures replicate those used in a previous publication [31]. See **S1 Movie**.

Experiment 2: LabGym2's outputs include the likelihood of each behavioral category per video frame on a 0-1 scale. The categories were initially the same as our proof-of-concept study in prairie voles [32]: aggression, chasing, being chased, approaching, sniffing, being sniffed, moving alone, idling alone, huddling. For the present study, aggression was ignored (replaced by manual annotations, as described below) and adaptations to other categories were made using MATLAB.

1) Sniffing into Pointing: This category merged three types of sniffing (face-to-face, face-to-body, anogenital) and approaching behaviors. This was renamed to a generic term, "pointing", as freezing-like behaviors that typically occurred after aggressive bouts (**S2 Movie**) were often misclassified as "sniffing" under LabGym2's spatiotemporal patterning. Neural network refinement and deeper ethological exploration were outside our scope (e.g., sub-classification of sniffing, sequencing of peri-aggression postures).
2) Behaving alone: This category merged "moving alone" and "idling alone" (this latter included self-grooming). In-depth exploration of these solitary behaviors was outside our scope, hence the creation of this generic category. Frames were set to zero

614 likelihood of “behaving alone” if only one animal was classified under this category,
615 making it a full-dyad category (see purple curves in **Fig 3**).
616 3) Huddling: Same as the previous proof-of-concept study in 10-min recordings [32], but
617 with one correction that we found necessary in the present 4-h recordings. During
618 intense body contact, the identities of both animals sometimes merged into one,
619 causing “huddling” to be misclassified as “idling alone”. Frames with this issue we re-
620 classified as huddling. Frames were set to zero likelihood of “huddling” if only one
621 animal was classified under this category, making it a full-dyad category (see purple
622 curves in **Fig 3**).
623 After these adaptations, likelihood values were converted into a vector of integer labels
624 using a winner-takes-all approach. Finally, frames manually classified as “attacking” and “being
625 attacked” were superimposed on that vector of labels. For final quantification (explained next),
626 the focal roles of chasing, attacking, and pointing were analyzed without their mirroring
627 counterparts (i.e., being chased, being attacked, being pointed at), thus minimizing redundancy
628 in the figures.
629
630 ***Final data processing and statistical analysis per figure***
631
632 **Figs 2 and 3**: Time series data obtained from the behavioral decomposition (Experiment
633 1) and behavioral annotation (Experiment 2) methods above were analyzed, with each data
634 point corresponding to one video frame of a single animal. These data points were binned and
635 smoothed on a per-animal basis: the 72-h recordings of Experiment 1 were averaged into 1-h
636 bins (total of 72 bins) and the 4-h recordings of Experiment 2 were averaged into 3-min bins
637 (total of 80 bins), both followed by a 6-bin moving mean window. The binned data were then
638 plotted as +/- standard error curves comparing males vs. females overall, males vs. females
639 within major dyad groups (matched or mixed), males vs. females within dyad sub-groups (Ctrl-

640 Ctrl, ELSD-ELSD, Ctrl-ELSD, ELSD-Ctrl), and matched vs. mixed dyads within each sex. These
641 comparisons were performed comprehensively across behavioral variables, allowing to identify
642 sex or dyad type differences with both: (1) behavioral variable specificity (in which behavioral
643 variables the dyad type precipitated or amplified differences?); and (2) temporal specificity (at
644 which time bins did these differences emerge?). Statistical comparisons were made using two-
645 way ANOVA with time bins as repeated measures, followed by Tukey's post-hoc tests per time
646 bin. The main statistical effects (sex, time, interaction) are reported in **Tables 1 and 2** and
647 significant post-hoc differences are depicted as bold lines along the x-axes in **Figs 2 and 3**.
648 Distributions per repeated measure passed the Kolmogorov-Smirnov normality test.

649 **Fig 4**: Experiments 1 and 2 were performed in different environments (divided and
650 undivided cohabitation), 3-4 days apart. The animals and dyad assignments were the same
651 between experiments, allowing for correlation analyses among all eight variables from the two
652 experiments. To investigate this, behavioral variables were averaged across the entirety of each
653 experiment, resulting in eight averages per animal. These averages were then grouped by sex
654 and major dyad type (males or females from matched or mixed), forming four animal x variable
655 arrays. Linear correlations within each sex and dyad type group were calculated, producing
656 matrices with correlation coefficients (R) and corresponding P values. Key correlations were
657 illustrated as scatter plots with linear fits in **Fig 4A-B**, while the R and P value matrices
658 themselves were illustrated with a color code in **Fig 4C**. Distributions per variable passed the
659 Kolmogorov-Smirnov normality test.

660 **Fig 5A-B**: Behavior transition probabilities were computed using 1-s time bins, matching
661 the approximate timescale of prairie vole behaviors, including chasing and aggression bouts.
662 For Experiment 1, continuous DeepLabCut-based variables of direction and distance to divider
663 were averaged per time bin and discretized into categorical vectors (number of elements =
664 number of time bins), enabling transition probability analysis. For discretization, direction to
665 divider was converted from a -1 to 1 scale into "toward" vs. "opposite", whereas distance to

divider was converted from a centimeter scale into “near” vs. “away”. These categories were combined into a four-category vector (toward-near, opposite-near, toward-away, opposite-away), one per animal. Then each dyad had a “time t” animal and a “time t+1” animal assignment, one iteration per sex directionality (male-then-female, female-then-male). Each of these iterations resulted in a 4 x 4 adjacency matrix (4 = number of behavioral categories), with rows representing “time t” behaviors, columns representing “time t+1” behaviors, and values indicating probabilities. Multiple such adjacency matrices were created, grouped by both sex directionality and dyad type. Specifically for the illustrations in **Fig 5A**, adjacency matrices were averaged across the dyads of each group and plotted as directed graphs. The edges of these graphs were coded by both weight and grayscale: the thicker and darker the edge, the higher the transition probability. For quantification (**Fig 5B**) no averaging was applied. Instead, each adjacency matrix (one per dyad) was reshaped into a row vector containing all behavior pairs (“behavior in time t” and “behavior in time t+1”). These rows were then concatenated across dyads, creating dyad x behavior pair matrices. Finally, dyad x behavior pair matrices from matched and mixed dyads were statistically compared per sex directionality using two-way ANOVA with behavior pairs as repeated measures, followed by Tukey’s post-hoc tests per behavior pair. The main statistical effects (dyad type, behavior pair, interaction) are reported in **Table 3** and significant post-hoc differences are depicted as bold edges in **Fig 5B**. Distributions per repeated measure passed the Kolmogorov-Smirnov normality test.

Fig 5C-D: Similar methods were used for Experiment 2 with three differences: (1) LabGym2-based data were already in categorical form prior to analysis, eliminating the need for categorization; (2) each time bin (1 s) was assigned its most frequent category (winner-takes-all); and (3) this analysis included five behavioral categories (chasing, attacking, pointing, behaving alone, huddling), leading to 5 x 5 adjacency matrices.

Data and code availability

The behavior tracking software (LabGym) and the training dataset for prairie voles are both available on GitHub (https://github.com/umyelab/LabGym). Processed post-tracking data, as well as code for figure plotting and statistical analysis are available to peer reviewers via private link on figshare.

Supporting information

S1 Movie. Decomposing behavioral variables in the divided cage

S2 Movie. Examples of behaviors in the undivided cage

Acknowledgements

This research was supported by the National Institute of Mental Health to B.O.W., M.M.L., L.S.B-J., C.E.J-T. (R01MH131592) and N.E.P.M. (F31MH136684), and the National Institute of Neurological Disorders and Stroke to B.Y. (R01NS137222). We thank all lab colleagues for discussions.

Author contributions

Conceptualization: Lezio S. Bueno-Junior, Noah E. P. Milman, Carolyn E. Jones-Tinsley, Miranda M. Lim, Brendon O. Watson.

Data curation: Lezio S. Bueno-Junior, Brendon O. Watson.

Formal analysis: Lezio S. Bueno-Junior.

Funding acquisition: Brendon O. Watson, Miranda M. Lim, Lezio S. Bueno-Junior, Carolyn E. Jones-Tinsley.

Investigation: Lezio S. Bueno-Junior.

Methodology: Lezio S. Bueno-Junior, Carolyn E. Jones-Tinsley, Noah E. P. Milman.

Project administration: Brendon O. Watson, Miranda M. Lim.

Software: Lezio S. Bueno-Junior, Yujia Hu, Bing Ye, Anjesh Ghimire.

Resources: Carolyn E. Jones-Tinsley, Peyton T. Wickham, Brendon O. Watson, Miranda M. Lim.

Supervision: Brendon O. Watson, Miranda M. Lim.

Visualization: Lezio S. Bueno-Junior.

Writing – original draft: Lezio S. Bueno-Junior.

Writing – review & editing: Noah E. P. Milman, Brendon O. Watson, Miranda M. Lim, Carolyn E. Jones-Tinsley, Anjesh Ghimire, Peyton T. Wickham, Yujia Hu, Bing Ye.

Declaration of interests

The authors declare no competing interests.

References

1. Locke KD, Horowitz LM. Satisfaction in interpersonal interactions as a function of similarity in level of dysphoria. J Pers Soc Psychol. 1990;58: 823–831. doi:10.1037/0022-3514.58.5.823

740 2. Bauminger N, Solomon M, Aviezer A, Heung K, Brown J, Rogers SJ. Friendship in high-
741 functioning children with Autism Spectrum Disorder: Mixed and non-mixed dyads. J Autism
742 Dev Disord. 2008;38: 1211–1229. doi:10.1007/s10803-007-0501-2

743 3. Petrina N, Carter M, Stephenson J, Sweller N. Perceived friendship quality of children with
744 Autism Spectrum Disorder as compared to their peers in mixed and non-mixed dyads. J
745 Autism Dev Disord. 2016;46: 1334–1343. doi:10.1007/s10803-015-2673-5

746 4. Crompton CJ, Sharp M, Axbey H, Fletcher-Watson S, Flynn EG, Ropar D. Neurotype-
747 matching, but not being autistic, influences self and observer ratings of interpersonal
748 rapport. Front Psychol. 2020;11: 586171. doi:10.3389/fpsyg.2020.586171

749 5. Morrison KE, DeBrabander KM, Jones DR, Faso DJ, Ackerman RA, Sasson NJ. Outcomes
750 of real-world social interaction for autistic adults paired with autistic compared to typically
751 developing partners. Autism. 2020;24: 1067–1080. doi:10.1177/1362361319892701

752 6. Bolis D, Lahnakoski JM, Seidel D, Tamm J, Schilbach L. Interpersonal similarity of autistic
753 traits predicts friendship quality. Soc Cogn Affect Neurosci. 2021;16: 222–231.
754 doi:10.1093/scan/nsaa147

755 7. Cunningham CE, Siegel LS. Peer interactions of normal and attention-deficit-disordered
756 boys during free-play, cooperative task, and simulated classroom situations. J Abnorm
757 Child Psychol. 1987;15: 247–268. doi:10.1007/BF00916353

758 8. Clark ML, Cheyne JA, Cunningham CE, Siegel LS. Dyadic peer interaction and task
759 orientation in attention-deficit-disordered children. J Abnorm Child Psychol. 1988;16: 1–15.
760 doi:10.1007/BF00910496

761 9. Schuldt JP, Chabris CF, Woolley AW, Hackman JR. Confidence in dyadic decision making:
762 The role of individual differences. J Behav Decis Mak. 2017;30: 168–180.
763 doi:10.1002/bdm.1927

764 10. Crompton CJ, Ropar D, Evans-Williams CV, Flynn EG, Fletcher-Watson S. Autistic peer-
765 to-peer information transfer is highly effective. Autism. 2020;24: 1704–1712.
766 doi:10.1177/1362361320919286

767 11. Crompton CJ, Foster SJ, Wilks CEH, Dodd M, Efthimiou TN, Ropar D, et al. Information
768 transfer within and between autistic and non-autistic people. Nat Hum Behav. 2025 [cited
769 22 May 2025]. doi:10.1038/s41562-025-02163-z

770 12. Georgescu AL, Koeroglu S, Hamilton AFDC, Vogeley K, Falter-Wagner CM, Tschacher W.
771 Reduced nonverbal interpersonal synchrony in autism spectrum disorder independent of
772 partner diagnosis: a motion energy study. Mol Autism. 2020;11: 11. doi:10.1186/s13229-
773 019-0305-1

774 13. Rifai OM, Fletcher-Watson S, Jiménez-Sánchez L, Crompton CJ. Investigating markers of
775 rapport in autistic and nonautistic interactions. Autism Adulthood. 2022;4: 3–11.
776 doi:10.1089/aut.2021.0017

777 14. Estrugo Y, Bar Yehuda S, Bauminger-Zviely N. Pathways to peer interaction in ASD and
778 TD through individual and dyadic joint-action motor abilities. Front Psychol. 2023;14:
779 1234376. doi:10.3389/fpsyg.2023.1234376

780 15. Geelhand P, Papastamou F, Jaspard S, Kissine M. Autistic adults display different verbal
781 behavior only in mixed-neurotype interactions: Evidence from a referential communication
782 task. Autism. 2024; 13623613241298376. doi:10.1177/13623613241298376

783 16. Koehler JC, Dong MS, Bierlich AM, Fischer S, Späth J, Plank IS, et al. Machine learning
784 classification of autism spectrum disorder based on reciprocity in naturalistic social
785 interactions. Transl Psychiatry. 2024;14: 76. doi:10.1038/s41398-024-02802-5

786 17. McNaughton KA, Moss A, Yarger HA, Redcay E. Smiling synchronization predicts
787 interaction enjoyment in peer dyads of autistic and neurotypical youth. Autism. 2024;28:
788 2754–2767. doi:10.1177/13623613241238269

789 18. Moreau Q, Brun F, Ayrolles A, Nadel J, Dumas G. Distinct social behavior and inter-brain
790 connectivity in Dyads with autistic individuals. Soc Neurosci. 2024;19: 124–136.
791 doi:10.1080/17470919.2024.2379917

792 19. Oates M, Bean A, Kickbusch R, Sauer S. Extending double empathy: Effects of neurotype-
793 matching on communication success in an expository context. Am J Speech Lang Pathol.
794 2024;33: 2364–2377. doi:10.1044/2024_AJSLP-23-00393

795 20. Zhao H, Zhang C, Tao R, Wang M, Yin Y, Xu S. Dyadic similarity in social value orientation
796 modulates hyper-brain network dynamics during interpersonal coordination: An fNIRS-
797 based hyperscanning study. Brain Topogr. 2025;38: 15. doi:10.1007/s10548-024-01092-w

798 21. Milton DEM. On the ontological status of autism: the ‘double empathy problem.’ Disabil
799 Soc. 2012;27: 883–887. doi:10.1080/09687599.2012.710008

800 22. Anderson C, Wood CI, Franklin L, Iampieri A, Sarsony C. “Getting Autism”: Educators,
801 parents, and autistic adults and teens reflect on the importance of teachers who
802 understand. J Autism Dev Disord. 2024 [cited 2 Apr 2025]. doi:10.1007/s10803-024-
803 06353-y

804 23. Rachanska PE. The Double Empathy Problem: An exploration of trans-neurotype attitudes
805 on autistic–non-autistic social interactions and communication. Adv Neurodev Disord. 2025
806 [cited 2 Apr 2025]. doi:10.1007/s41252-024-00435-9

807 24. Nicolini C, Fahnestock M. The valproic acid-induced rodent model of autism. Exp Neurol.
808 2018;299: 217–227. doi:10.1016/j.expneurol.2017.04.017

809 25. Delling JP, Boeckers TM. Comparison of SHANK3 deficiency in animal models:
810 phenotypes, treatment strategies, and translational implications. J Neurodevelop Disord.
811 2021;13: 55. doi:10.1186/s11689-021-09397-8

812 26. Kabra M, Robie AA, Rivera-Alba M, Branson S, Branson K. JAABA: interactive machine
813 learning for automatic annotation of animal behavior. Nat Methods. 2013;10: 64–67.
814 doi:10.1038/nmeth.2281

815 27. Romero-Ferrero F, Bergomi MG, Hinz RC, Heras FJH, De Polavieja GG. idtracker.ai:
816 tracking all individuals in small or large collectives of unmarked animals. Nat Methods.
817 2019;16: 179–182. doi:10.1038/s41592-018-0295-5

818 28. Lauer J, Zhou M, Ye S, Menegas W, Schneider S, Nath T, et al. Multi-animal pose
819 estimation, identification and tracking with DeepLabCut. Nat Methods. 2022;19: 496–504.
820 doi:10.1038/s41592-022-01443-0

821 29. Pereira TD, Tabris N, Matsliah A, Turner DM, Li J, Ravindranath S, et al. SLEAP: A deep
822 learning system for multi-animal pose tracking. Nat Methods. 2022;19: 486–495.
823 doi:10.1038/s41592-022-01426-1

824 30. Jones CE, Opel RA, Kaiser ME, Chau AQ, Quintana JR, Nipper MA, et al. Early-life sleep
825 disruption increases parvalbumin in primary somatosensory cortex and impairs social
826 bonding in prairie voles. Sci Adv. 2019;5: eaav5188. doi:10.1126/sciadv.aav5188

827 31. Bueno-Junior LS, Jones-Tinsley CE, Milman NEP, Wickham PT, Watson BO, Lim MM.
828 Early-life sleep disruption impairs subtle social behaviours in prairie voles: a pose-
829 estimation study. R Soc Open Sci. 2023;10: 230700. doi:10.1098/rsos.230700

830 32. Goss K, Bueno-Junior LS, Stangis K, Ardoin T, Carmon H, Zhou J, et al. Quantifying social
831 roles in multi-animal videos using subject-aware deep-learning. 2024.
832 doi:10.1101/2024.07.07.602350

833 33. Jones-Tinsley CE, Olson RJ, Mader M, Wickham PT, Gutowsky K, Wong C, et al. Early life
834 sleep disruption has long lasting, sex specific effects on later development of sleep in
835 prairie voles. Neurobiology of Sleep and Circadian Rhythms. 2023;14: 100087.
836 doi:10.1016/j.nbscr.2022.100087

837 34. Jones CE, Chau AQ, Olson RJ, Moore C, Wickham PT, Puranik N, et al. Early life sleep
838 disruption alters glutamate and dendritic spines in prefrontal cortex and impairs cognitive
839 flexibility in prairie voles. Curr Res Neurobiol. 2021;2: 100020.
840 doi:10.1016/j.crneur.2021.100020

841 35. Milman NEP, Tinsley CE, Raju RM, Lim MM. Loss of sleep when it is needed most –
842 Consequences of persistent developmental sleep disruption: A scoping review of rodent
843 models. Neurobiol Sleep Circadian Rhythms. 2023;14: 100085.
844 doi:10.1016/j.nbscr.2022.100085

845 36. Bruni O, Breda M, Mammarella V, Mogavero MP, Ferri R. Sleep and circadian
846 disturbances in children with neurodevelopmental disorders. Nat Rev Neurol. 2025;21:
847 103–120. doi:10.1038/s41582-024-01052-9

848 37. Vargas C, Paoletti D, De Stasio S, Berenguer C. Sleep disturbances in autistic children
849 and adolescents: A systematic review and meta-analysis of randomized controlled trials.
850 Autism. 2025;29: 1661–1673. doi:10.1177/13623613251319391

851 38. Pugsley K, Scherer SW, Bellgrove MA, Hawi Z. Environmental exposures associated with
852 elevated risk for autism spectrum disorder may augment the burden of deleterious de novo
853 mutations among probands. Mol Psychiatry. 2022;27: 710–730. doi:10.1038/s41380-021-
854 01142-w

855 39. Covington LB, Patterson F, Hale LE, Teti DM, Cordova A, Mayberry S, et al. The
856 contributory role of the family context in early childhood sleep health: A systematic review.
857 Sleep Health. 2021;7: 254–265. doi:10.1016/j.sleh.2020.11.010

858 40. Reiter J, Ramagopal M, Gileles-Hillel A, Forno E. Sleep disorders in children with asthma.
859 Pediatr Pulmonol. 2022;57: 1851–1859. doi:10.1002/ppul.25264

860 41. Miot S, Chancel R, Peries M, Crepiat S, Couderc S, Pernon E, et al. Multimorbidity
861 patterns and subgroups among autistic adults with intellectual disability: Results from the
862 EFAAR study. Autism. 2023;27: 762–777. doi:10.1177/13623613221121623

863 42. Sharma SR, Gonda X, Tarazi FI. Autism Spectrum Disorder: Classification, diagnosis and
864 therapy. Pharmacol Ther. 2018;190: 91–104. doi:10.1016/j.pharmthera.2018.05.007

865 43. Hirota T, King BH. Autism Spectrum Disorder: A Review. JAMA. 2023;329: 157.
866 doi:10.1001/jama.2022.23661

867 44. Poncela-Casasnovas J, Gutiérrez-Roig M, Gracia-Lázaro C, Vicens J, Gómez-Gardeñes J,
868 Perelló J, et al. Humans display a reduced set of consistent behavioral phenotypes in
869 dyadic games. Sci Adv. 2016;2: e1600451. doi:10.1126/sciadv.1600451

870 45. Zapata-Fonseca L, Dotov D, Fossion R, Froese T. Time-series analysis of embodied
871 interaction: Movement variability and complexity matching as dyadic properties. Front
872 Psychol. 2016;7. doi:10.3389/fpsyg.2016.01940

873 46. Endevelt-Shapira Y, Perl O, Ravia A, Amir D, Eisen A, Bezalel V, et al. Altered responses
874 to social chemosignals in autism spectrum disorder. Nat Neurosci. 2018;21: 111–119.
875 doi:10.1038/s41593-017-0024-x

876 47. Parkinson C, Kleinbaum AM, Wheatley T. Similar neural responses predict friendship. Nat
877 Commun. 2018;9: 332. doi:10.1038/s41467-017-02722-7

878 48. Hyon R, Youm Y, Kim J, Chey J, Kwak S, Parkinson C. Similarity in functional brain
879 connectivity at rest predicts interpersonal closeness in the social network of an entire
880 village. Proc Natl Acad Sci U S A. 2020;117: 33149–33160. doi:10.1073/pnas.2013606117

881 49. Ravreby I, Snitz K, Sobel N. There is chemistry in social chemistry. Sci Adv. 2022;8:
882 eabn0154. doi:10.1126/sciadv.abn0154

883 50. Robinson EB, Lichtenstein P, Anckarsäter H, Happé F, Ronald A. Examining and
884 interpreting the female protective effect against autistic behavior. Proc Natl Acad Sci U S
885 A. 2013;110: 5258–5262. doi:10.1073/pnas.1211070110

886 51. Werling DM, Geschwind DH. Sex differences in autism spectrum disorders. Curr Opin
887 Neurol. 2013;26: 146–153. doi:10.1097/WCO.0b013e32835ee548

888 52. Hull L, Mandy W, Petrides K. Behavioural and cognitive sex/gender differences in autism
889 spectrum condition and typically developing males and females. Autism. 2017;21: 706–
890 727. doi:10.1177/1362361316669087

891 53. Brusman LE, Protter DSW, Fultz AC, Paulson MU, Chapel GD, Elges IO, et al. Emergent
892 intra-pair sex differences and organized behavior in pair bonded prairie voles (Microtus
893 ochrogaster). Genes Brain Behav. 2022;21: e12786. doi:10.1111/gbb.12786

894 54. Flavell SW, Gogolla N, Lovett-Barron M, Zelikowsky M. The emergence and influence of
895 internal states. Neuron. 2022;110: 2545–2570. doi:10.1016/j.neuron.2022.04.030

896 55. Vahaba DM, Halstead ER, Donaldson ZR, Ahern TH, Beery AK. Sex differences in the
897 reward value of familiar mates in prairie voles. Genes Brain Behav. 2022;21: e12790.
898 doi:10.1111/gbb.12790

899 56. Bohnslav JP, Wimalasena NK, Clausing KJ, Dai YY, Yarmolinsky DA, Cruz T, et al.
900 DeepEthogram, a machine learning pipeline for supervised behavior classification from raw
901 pixels. eLife. 2021;10: e63377. doi:10.7554/eLife.63377

902 57. Kenkel W. Automated behavioral scoring: Do we even need humans? Ann N Y Acad Sci.
903 2023;1527: 25–29. doi:10.1111/nyas.15041

904

905

Figure legends

Fig 1. Overview of animal pairing and behavioral analysis. A. Early-life sleep disruption (ELSD) in prairie vole pups (post-natal days 14-21) generates phenotypes relevant to autism, as indicated by behavioral and cytoarchitectural evidence [30,34]. ELSD subjects and their controls were raised into adulthood in same-sex sibling groups under standard conditions. The adults were then assigned into matched and mixed opposite-sex dyads. **B.** Experiment 1: Male and female were filmed for 72 h while they interacted through a wire-mesh divider at the center of the cage. Cameras were positioned at an overhead angle and the animals were tracked using DeepLabCut [28], yielding cage-referenced behavioral variables. A similar method was utilized in a previous study [31] but without directly investigating dyad type. **C.** Experiment 2: After 3-4 days of single housing in the vivarium, the same dyads were placed back together into the recording setup, this time for 4 h and without the divider. This resulted in a different kind of dataset comprising partner-referenced social role categories, annotated using LabGym2 [32] and manual validation (see Methods).

Fig 2. Experiment 1: Mixed dyads showed exacerbated sex differences in body orientation. A. Time series data (72 h, 1-h bins) showing sex differences in direction to divider across all dyads. Males spent more time toward the divider than females throughout the recordings. The curves represent mean +/- standard error aggregated across animals, regardless of individual dyad assignments. The black bars on the x-axes represent posthoc differences, after two-way ANOVA with time bins as repeated measures. **B.** Sex differences in direction to divider were more pronounced in mixed dyads (highlighted with gray background). Distance to divider and locomotion speed were less sensitive to dyad type, illustrating that behavioral decomposition was important to capture the effects shown here. **C.** Further specification into the four dyad subtypes. Sex differences in direction to divider were confined to

932 the mixed-dyad subtypes (Ctrl-ELSD, ELSD-Ctrl). Additional smaller effects were observed in
933 distance to divider and locomotion speed, specific to each mixed-dyad subtype. **D.** Same
934 groupings as panel B but comparing matched and mixed dyads within each sex. The tendency
935 to behave toward the divider was higher in males and further increased in mixed-dyad males.
936 See **Table 1** for statistics and **S1 Movie**.
937
938 **Fig 3. Experiment 2: Mixed dyads showed higher female-to-male aggression. A.** Time
939 series data (4 h, 3-min bins) showing sex differences in the likelihood of chasing and attacking
940 across all dyads. Females were more likely to chase and attack than males, especially in the
941 initial hour of recording. The curves represent mean +/- standard error aggregated across
942 animals, regardless of individual dyad assignments. The black bars on the x-axes represent
943 posthoc differences, after two-way ANOVA with time bins as repeated measures. Inset plots
944 show probability within the first hour. **B.** Sex differences in the likelihood of chasing and
945 attacking were more pronounced in mixed dyads (highlighted by gray background). Pointing
946 behaviors, including face-to-face, face-to-body and anogenital sniffing, showed no sex or dyad
947 type specificity, making them useful comparators (see Methods for details). The role-unspecific
948 categories of alone and huddling were more dominant and mutually exclusive, illustrating the
949 transition from high activity (periods of moving and idling alone punctuated by chasing,
950 aggression and sniffing bouts) to low activity (periods of continuous huddling). **C.** Further
951 specification into the four dyad subtypes. Sex differences in the likelihood of chasing and
952 attacking were stronger in the mixed-dyad subtypes (Ctrl-ELSD, ELSD-Ctrl). **D.** Same groupings
953 as panel B but comparing matched and mixed dyads within each sex. Mixed-dyad females were
954 more likely to chase and attack than matched-dyad females. See **Table 2** for statistics and **S2**
955 **Movie**.
956

957 **Fig 4. Linking divided cohabitation to undivided cohabitation: Neurotype matching**
958 **affected correlations among behaviors. A.** Correlations between the most sensitive variable
959 from Experiment 1 (72-h divided cohabitation), direction to divider (x-axes), and behavior
960 probabilities from Experiment 2 (4-h undivided cohabitation; y-axes), averaged per male
961 individual (data points). **B.** Same but for females. Significant correlations revealed further
962 distinctions between dyad types, highlighted by gray backgrounds. Matched-dyad females
963 formed an affiliation-driven spectrum: a higher tendency to behave toward the divider in
964 Experiment 1 correlated with higher sociability 3-4 days later, in Experiment 2 (lower likelihood
965 to attack and behave alone, higher likelihood to huddle). This pattern was absent in mixed-dyad
966 females; instead, they exhibited a positive correlation between direction to divider and chasing
967 behavior. **C.** Comprehensive view of all correlation pairs. R and P values are coded by color and
968 square size, respectively. Note that the scatter plots in panels A-B correspond to the leftmost
969 column of each correlation matrix.
970
971 **Fig 5. Female-to-male behavior transitions differed between matched and mixed dyads.**
972 **A.** Data from Experiment 1 (divided cohabitation). Direction and distance to divider were time-
973 binned (1-s), categorized (toward-near, opposite-near, toward-away, opposite-away), and
974 analyzed as male-to-female and female-to-male transition probability matrices (see Methods).
975 Directed graphs (averaged across dyads) illustrate patterns that varied with both dyad type and
976 sex directionality. **B.** Quantitative comparisons between dyad types within each sex
977 directionality, using one transition matrix per dyad, rather than the averages in panel A.
978 Behavior pairs were used as repeated measures in this analysis (see Methods). Self-loops were
979 excluded to focus on inter-behavior relationships. The directed graphs highlight which
980 transitions differed statistically between dyad types. The scatter plots exemplify the distributions
981 underlying each transition edge (each data point is a dyad). Mean +/- standard deviation bars
982 accompany the scatter plots. **C-D.** Same as panels A-B but from Experiment 2 (undivided

983 cohabitation). Overall, these patterns suggest that matched dyads showed more variation in
984 body re-orientation behaviors between the females and males, as well as a higher likelihood of
985 female chasing leading to huddling, among other interpretations. See Results and Discussion.
986 See **Table 3** for statistics.

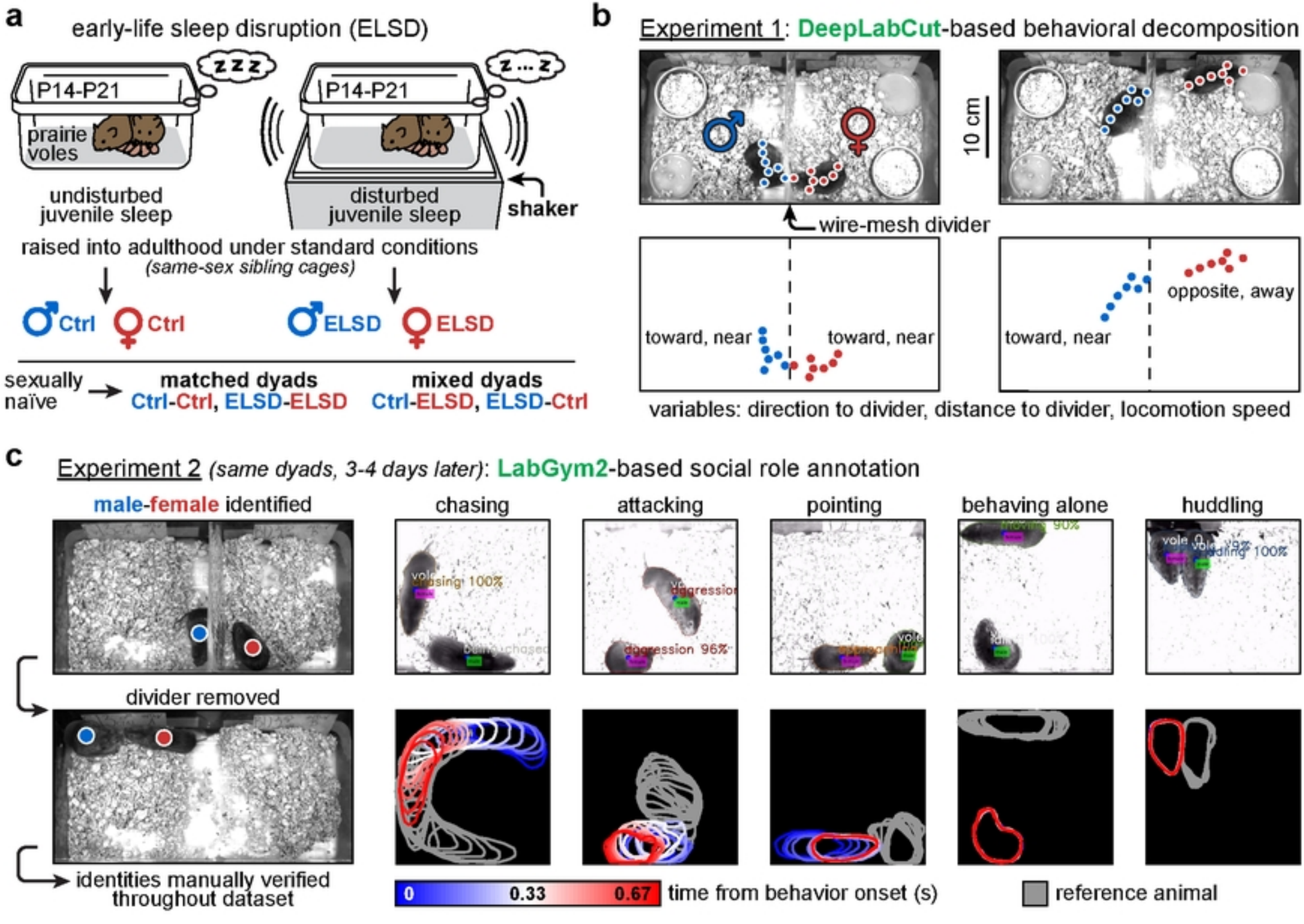
a
early-life sleep disruption (ELSD)
P14-P21
prairie voles
undisturbed juvenile sleep
P14-P21
disturbed juvenile sleep
shaker
raised into adulthood under standard conditions
(same-sex sibling cages)
Ctrl
Ctrl
ELSD
ELSD
sexually naïve
matched dyads
Ctrl-Ctrl, ELSD-ELSD
mixed dyads
Ctrl-ELSD, ELSD-Ctrl
b
Experiment 1: DeepLabCut-based behavioral decomposition
10 cm
wire-mesh divider
toward, near
toward, near
toward, near
opposite, away
variables: direction to divider, distance to divider, locomotion speed
c
Experiment 2 (same dyads, 3-4 days later): LabGym2-based social role annotation
male-female identified
chasing
attacking
pointing
behaving alone
huddling
divider removed
identities manually verified throughout dataset
0
0.33
0.67
time from behavior onset (s)
reference animal

Figure 1

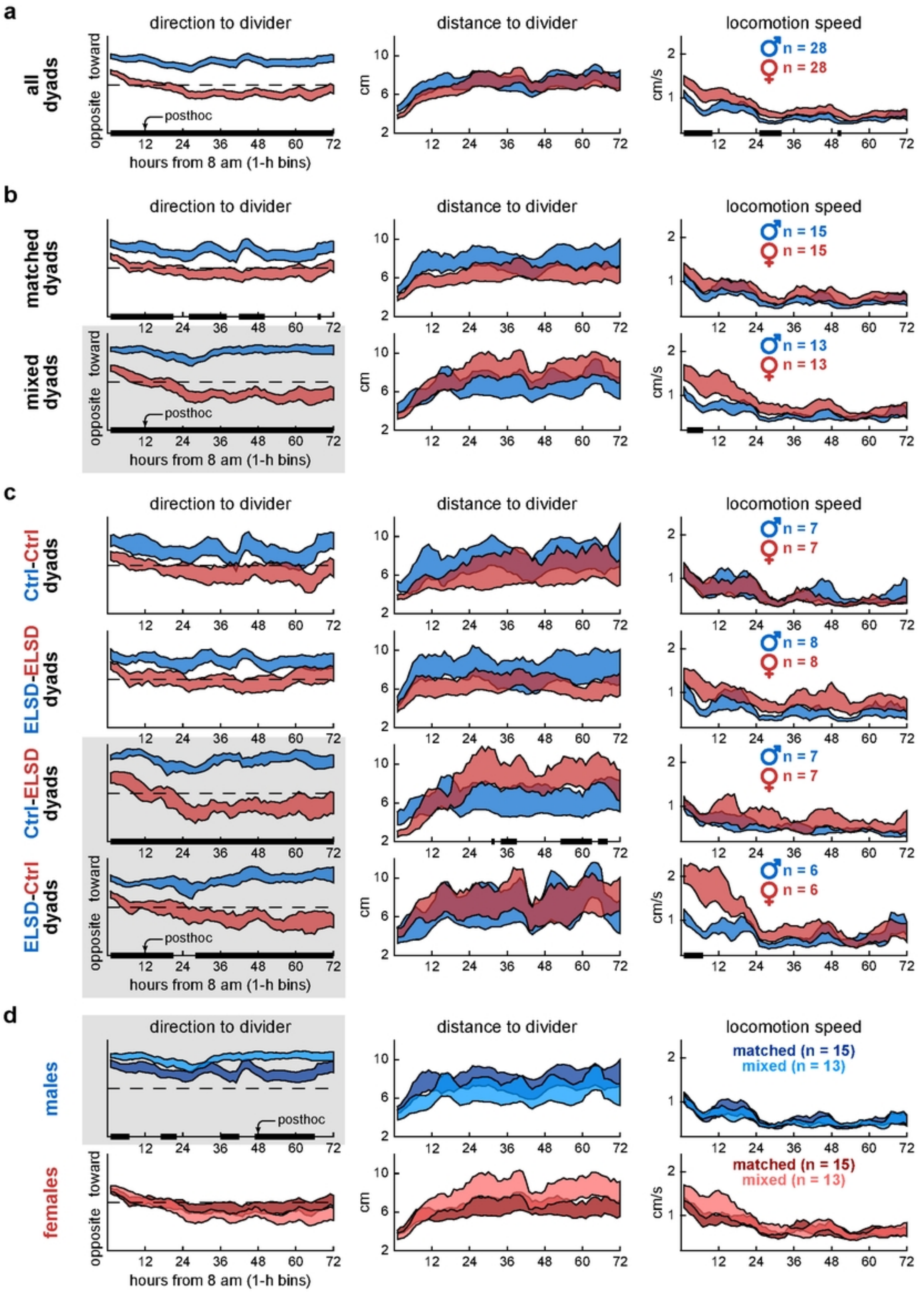
a
all dyads
direction to divider
distance to divider
locomotion speed
toward
opposite
posthoc
cm
cm/s
♂ n = 28
♀ n = 28
hours from 8 am (1-h bins)
b
matched dyads
mixed dyads
♂ n = 15
♀ n = 15
♂ n = 13
♀ n = 13
c
Ctrl-Ctrl dyads
ELSD-ELSD dyads
Ctrl-ELSD dyads
ELSD-Ctrl dyads
♂ n = 7
♀ n = 7
♂ n = 8
♀ n = 8
♂ n = 7
♀ n = 7
♂ n = 6
♀ n = 6
d
males
females
matched (n = 15)
mixed (n = 13)

Figure 2

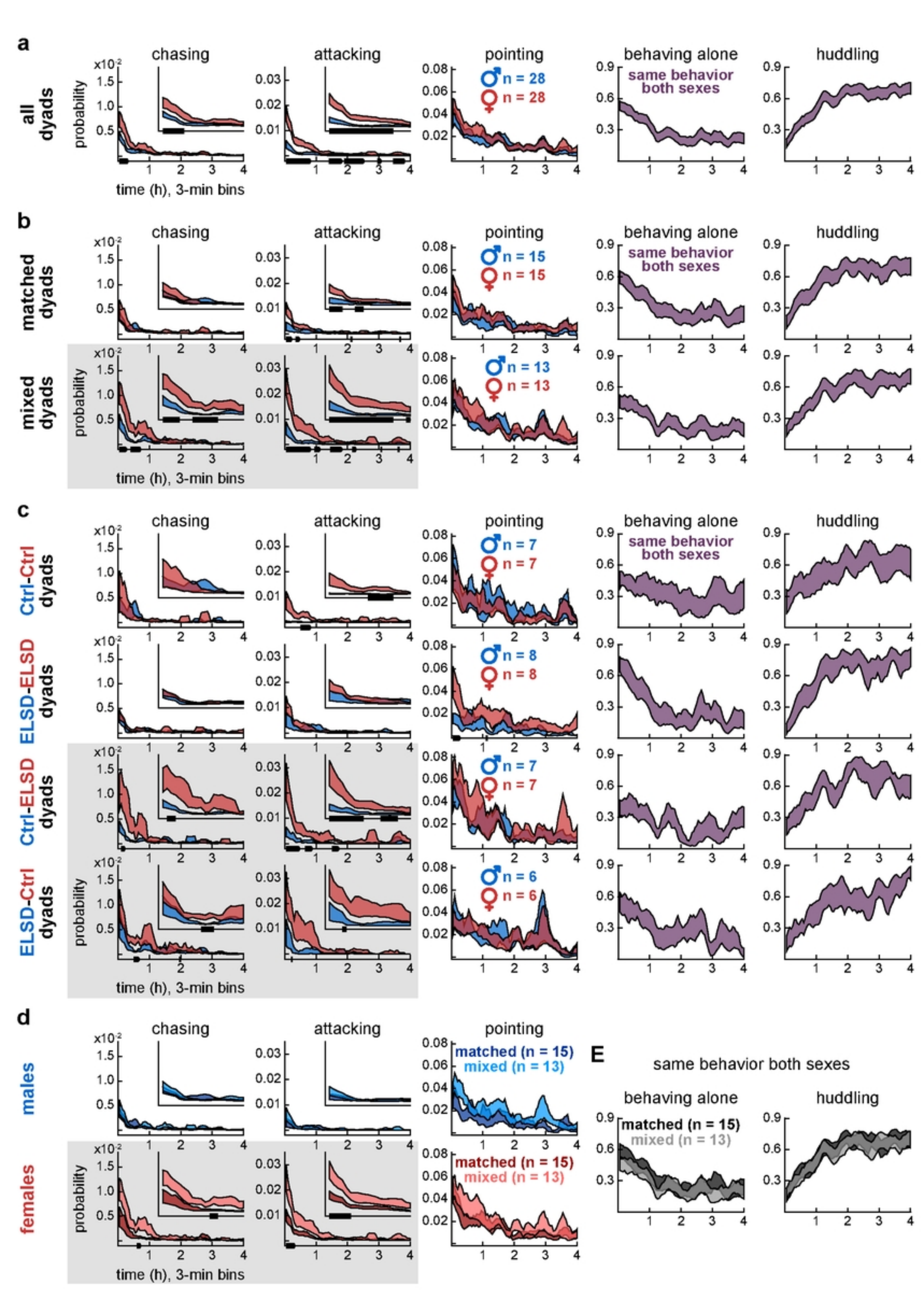
a
all dyads
chasing
attacking
pointing
behaving alone
huddling
probability
time (h), 3-min bins
n = 28
n = 28
same behavior both sexes
b
matched dyads
mixed dyads
n = 15
n = 15
n = 13
n = 13
c
Ctrl-Ctrl dyads
ELSD-ELSD dyads
Ctrl-ELSD dyads
ELSD-Ctrl dyads
n = 7
n = 7
n = 8
n = 8
n = 7
n = 7
n = 6
n = 6
d
males
females
matched (n = 15)
mixed (n = 13)
E
same behavior both sexes

Figure 3

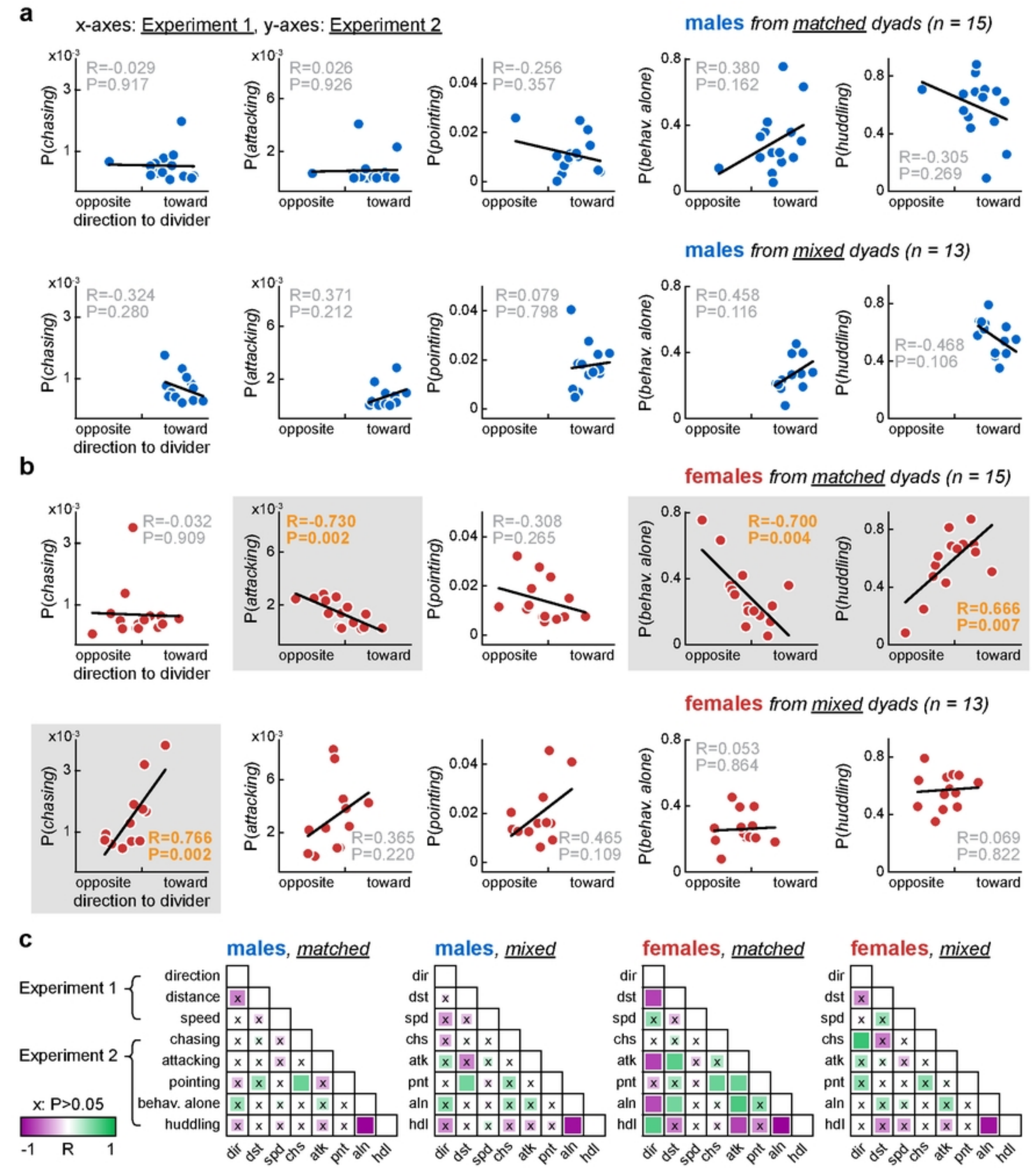
a
x-axes: Experiment 1, y-axes: Experiment 2
males from matched dyads (n = 15)
R=-0.029 P=0.917
R=0.026 P=0.926
R=-0.256 P=0.357
R=0.380 P=0.162
R=-0.305 P=0.269
males from mixed dyads (n = 13)
R=-0.324 P=0.280
R=0.371 P=0.212
R=0.079 P=0.798
R=0.458 P=0.116
R=-0.468 P=0.106
P(chasing)
P(attacking)
P(pointing)
P(behav. alone)
P(huddling)
opposite
toward
direction to divider
b
females from matched dyads (n = 15)
R=-0.032 P=0.909
R=-0.730 P=0.002
R=-0.308 P=0.265
R=-0.700 P=0.004
R=0.666 P=0.007
females from mixed dyads (n = 13)
R=0.766 P=0.002
R=0.365 P=0.220
R=0.465 P=0.109
R=0.053 P=0.864
R=0.069 P=0.822
c
males, matched
males, mixed
females, matched
females, mixed
Experiment 1
Experiment 2
direction
distance
speed
chasing
attacking
pointing
behav. alone
huddling
dir
dst
spd
chs
atk
pnt
aln
hdl
x: P>0.05
-1
R
1

Figure 4

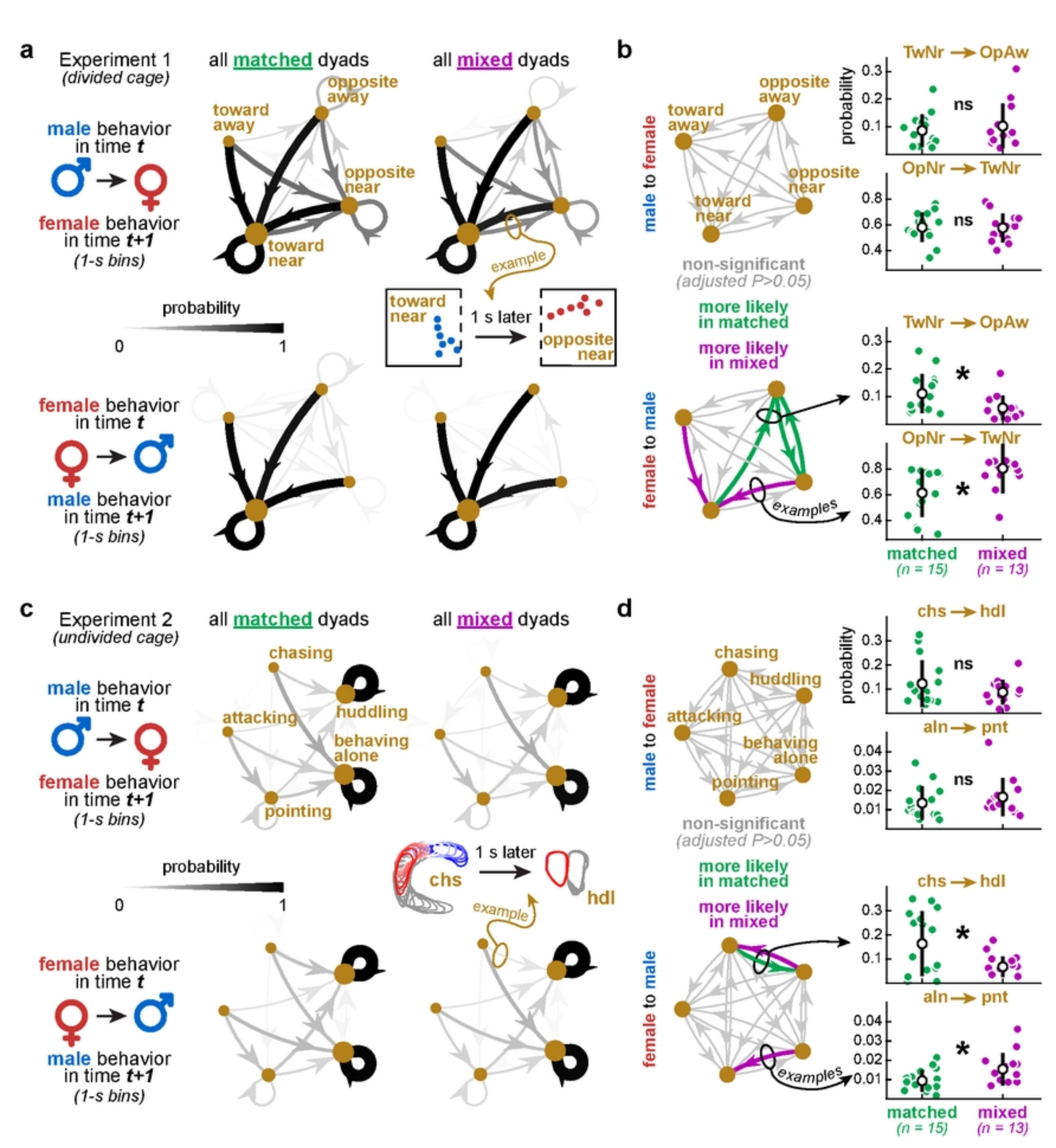
a
Experiment 1
(divided cage)
all matched dyads
all mixed dyads
male behavior in time t
female behavior in time t+1
(1-s bins)
toward away
opposite away
opposite near
toward near
example
toward near
1 s later
opposite near
probability
0
1
female behavior in time t
male behavior in time t+1
(1-s bins)
b
male to female
female to male
toward away
opposite away
opposite near
toward near
non-significant
(adjusted P>0.05)
more likely in matched
more likely in mixed
examples
probability
TwNr → OpAw
OpNr → TwNr
ns
*
matched
(n = 15)
mixed
(n = 13)
c
Experiment 2
(undivided cage)
all matched dyads
all mixed dyads
male behavior in time t
female behavior in time t+1
(1-s bins)
chasing
attacking
huddling
behaving alone
pointing
chs
1 s later
hdl
example
probability
0
1
female behavior in time t
male behavior in time t+1
(1-s bins)
d
male to female
female to male
chasing
huddling
attacking
behaving alone
pointing
non-significant
(adjusted P>0.05)
more likely in matched
more likely in mixed
examples
probability
chs → hdl
aln → pnt
ns
*
matched
(n = 15)
mixed
(n = 13)

Figure 5